Time and Frequency Transfer Using a WAAS Satellite with L1 and L5 Code and Carrier[*]

M.A. Weiss

Time and Frequency Division
NIST, Boulder, Colorado, U.S.A.
mweiss@boulder.nist.gov

P. Fenton

NovAtel Inc., Calgary, Alberta, Canada

E. Powers, A. Kropp, B. Fonville
USNO, Washington D.C., U.S.A.

R. Pelletier

NRC, Ottawa, Ontario, Canada

Abstract— **Two Wide Area Augmentation System (WAAS) satellites are now transmitting the standard L1 and L5 carriers and codes of the Global Positioning System (GPS), though with a five times higher data-bit rate. Since these are geostationary satellites, it is possible to aim a parabolic dish at one and obtain high-gain, low-multipath interference signals without interruption. Such high-gain dishes, along with appropriate GPS receivers, were set up at three timing laboratories in North America: the National Institute of Standards and Technology (NIST) in Boulder, Colorado, U.S.A., the United States Naval Observatory (USNO) in Washington D.C., U.S.A., and the National Research Council (NRC) in Ottawa, Ontario, Canada. We report the results of this experiment over a 104 d period: January 1 to April 14, 2008, though with several significant outages, and other clock/data problems.**

I. INTRODUCTION

As the uncertainties in primary atomic frequency standards drop below the 10^{-15} level, the community finds it increasingly difficult to compare standards among laboratories. Two-way satellite time and frequency transfer (TWSTFT) is now achieving comparison stabilities approximating 10^{-15} after 1 d [1]. GPS carrier phase time transfer techniques show potential for reaching similar levels [2] [2]. We explore a new technique here, using a high gain dish at a laboratory to receive signals from Wide Area Augmentation System (WAAS) satellites.

Two WAAS satellites are now transmitting the standard L1 and L5 carriers and codes of the Global Positioning System (GPS) [4]. The WAAS satellites and signals are operated by the US Federal Aviation Administration (FAA) and are used primarily to provide extra ranges and data to enable higher accuracy and integrity to GPS based aircraft navigation. The WAAS clock signal is transmitted from a ground control station, and steered to GPS time. Since these are geostationary satellites, it is possible to aim a parabolic dish at one and obtain high-gain, low-multipath interference signals without interruption. We can use an ionosphere-free combination of the L1 and L5 codes and carriers. With the large signal-to-noise ratio, there should be very few cycle slips, and very low tracking noise. Long observation intervals are possible, from days to weeks, leading the way to a method of providing continuous phase comparison between timing laboratories separated by thousands of kilometers. Since the dish antenna technology reverses the signal polarization, a left-hand circularly polarized antenna is required, tuned to the L1 and L5 frequencies and mounted at the focal point of the high-gain antenna. An alternative would be to use a Cassagrain reflector, which would allow use of a standard right-hand circularly polarized GPS antenna.

Such high-gain dishes, along with appropriate GPS receivers, were set up at three timing laboratories in North America: the National Institute of Standards and Technology (NIST) in Boulder, Colorado, U.S.A., the United States Naval Observatory (USNO) in Washington D.C., U.S.A., and the National Research Council (NRC) in Ottawa, Ontario, Canada. The labs measured their local Hydrogen masers against the signal from PRN#138, the WAAS signal from the Anik F1R. Because the time delays were not calibrated we study here only time stability. Data were taken over a 104 d period, though with some significant outages and other problems. Time and frequency transfer results were computed by use of these data.

II. ANALYSIS METHODS

Both code and carrier were used to optimize time transfer. The receivers gave a hardware indication of loss of lock. This indication and locations of large time gaps in the data set were used for cycle-slip detection. An estimator was used to determine and remove the size of cycle slips. For each interval of data with no slips, the ionosphere-free combination

---

[*]Contribution of U.S. government, not subject to copyright

of L1 and L5 code was averaged to determine the phase ambiguity of the ionosphere-free carrier. After thus removing the cycle ambiguity, the carrier data gave a measure of local reference clock time against WAAS system time. Note since there was no complete calibration of system delays, the results are for time transfer stability, not accuracy. The carrier measurements were significantly less noisy than the code measurements.

If $R1$ and $R5$ are the pseudo-range code measurements corresponding to frequencies $L1$ and $L5$ respectively, then the ionosphere-free combination R is given by

$$R = \frac{R1 \times L1^2}{L1^2 - L5^2} - \frac{R5 \times L5^2}{L1^2 - L5^2}. \qquad (1)$$

Equation (1) holds generally for any two frequencies, though for GPS we have, exactly, L1 = 154x10.23 MHz = 1.57542 GHz, L5 = 115x10.23 MHz = 1.17645 GHz.

In computing time transfer, estimates of the tropospheric delay and of the satellite positions are required. We used the transmitted satellite positions, though some refinement of this will be required in the future. We used the Hopfield model [5] to estimate the troposphere. We did not include it in the results, since the tropospheric model depends on station altitude and satellite elevation and azimuth, which hardly changed. For future work, we will use omni-directional dual-frequency GPS measurements from nearby receivers and precise point positioning (PPP) processing to estimate the actual troposphere correction. We may also use International GNSS Service (IGS) estimates of troposphere if available.

These data were differenced among the three laboratories, giving a comparison of the lab clocks. Unfortunately, there were significant periods of missing data. In addition there were steps in the clock time and frequency for some of the labs, and estimation problems in the early data segments. For these reasons we had to break the data into several intervals for analysis. We look at the modified Allan deviation (MDEV) [6] to characterize the frequency transfer capability of this technique in this initial study. We use the modified total deviation [7] to maximize confidence in long term.

III. RESULTS

We compared laboratory time standards using the WAAS code signals, and the WAAS carrier signals, though without calibrated delays. In both cases we used the ionosphere-free combination of L1 and L5. We present the comparison of NIST and USNO by WAAS code in Fig. 1, and by WAAS carrier in Fig. 2. We began processing data starting on MJD 54497. Data were lost from MJD 54520 to 54539. For analysis, we broke the data into two segments, before and after the data loss. The first segment was from MJD 54497 to 54520. The second was MJD 54539 to 54560. Fig. 3 and Fig. 4 show the MDEV and total MDEV of both the code and carrier for each of the data segments. The 1 d MDEV stability of carrier data for the second segment was our best result at 5×10^{-15}. Considering the amount of noise that is visible in Fig. 2, it seems promising as a first effort.

The carrier data follow the code data fairly well, but with much less noise. Hence for the rest of our discussion we plot only the carrier data. We see many deviations and anomalies in the data. A slope of -3/2 on an MDEV log-log plot indicates that white Phase Modulation (PM) dominates for those integration times, τ. A slope of -1 indicates flicker PM. A periodic variation appears as

$$\mathrm{mod}\,\sigma_y(\tau) = \frac{\sqrt{3}\,x_{pp}\sin^2(\pi f_m \tau)}{\sqrt{8\pi}\,f_m \tau^2}, \qquad (2)$$

where x_{pp} is the peak-peak amplitude of the periodic variation with frequency f_m. Thus a maximum in mod $\sigma_y(\tau)$ due to a periodic variation occurs when $\pi \cdot f_m \cdot \tau = \pi/2$, or when $f_m \cdot \tau = \frac{1}{2}$. Since the period is $1/f_m$, the maximum mod $\sigma_y(\tau)$ occurs when τ = half the period of variation [6].

We see evidence of periodic behavior with the maximum around $1-2 \times 10^4$ s. This appears to be a 12 hour periodic variation.

Larger variations appear in the form of time steps and wander. The two time scales are much more stable than the data in the plots. The clock difference MDEV is probably lower than the values in the figures. At all integration times, we are probably seeing WAAS transfer noise. One test of this is a comparison to GPS common-view (CV). CV uses L1 code only for time transfer. Multi-channel CV using IGS ionospheric estimates for NIST to USNO typically has Time deviation [8] (TDEV) levels of 300 ps at 1 d. We took 1 d averages of NIST-USNO CV data and subtracted them from the NIST-USNO WAAS carrier data in Fig. 5. Since the clocks are cancelled, and we are looking only at the difference of time transfer systems, we look at the TDEV and total TDEV of the data from the second segment, MJD 54539-54560, in Fig. 6. TDEV shows apparent flicker PM at 300 ps at 1 d, consistent with other results for CV. However, the values significantly worsen past 1 d. This implies that there are low frequency noise effects in either the WAAS carrier transfer or the GPS CV.

The possible causes of anomalies in the WAAS carrier time transfer are: differential ephemeris errors, tropospheric delay variations, unresolved slips in carrier phase, and local effects, such as changes in receiver delays, cables, or connectors. We find evidence of differential ephemeris errors, as we discuss below, causing jumps in time transfer values up to 15 ns. GPS carrier phase time transfer studies suggest worst-case tropospheric delay changes may reach a 1-3 ns over several days [9]. This may account for some of the TDEV values at times longer than 1 d. Typical local effects should not cause anomalies of this magnitude [10].

In the NIST-USNO carrier phase transfer data, a particularly large spike appears on MJD 54546. We investigated this in some detail. Fig. 7 shows the individual lab measurements that were used to compute the carrier time transfer. We see a walk-off of order 10 ns over about 50 minutes out to minute 1000 of the day. The walk has the same sign between NRC and USNO, but opposite sign at NIST.

Following this is a period with no measurements, followed by a spike in common across all three stations. This latter spike cancels in the time transfer. We conclude that we are seeing an increasing problem with the broadcast WAAS ephemeris, followed by a system outage, and then by a WAAS clock event upon resumption of the signal.

We look at results from NIST-NRC time transfer in Figs. 8-10. Clock events in Fig. 8 prevent analysis of a segment of data longer than about 10 d. Fig. 9 shows the longest, and last, segment available from this study, MJD 54521 - 54570. The τ^{-1} slope in Fig. 10 is consistent with a dominant noise type of flicker PM out past 1 d, with a stability of 10^{-14} at 1d. The linear frequency drift turns the MDEV slope up to τ^{+1} at about 10 d.

Clock events combined with loss of data yield the longest segment of the NRC-USNO data being from MJD 54539 to 54560. We show MDEV of these data in Fig. 11. As in Fig. 10, the results are consistent with a dominant noise type of flicker PM out past 1 d, with a stability of 10^{-14} at 1d. The flattening of MDEV as it approaches 10 d is probably due to linear frequency drift.

IV. CONCLUSIONS

This first use of two-frequency WAAS data for time transfer shows promise of reaching state-of-the-art time transfer capability. Future studies will need a better ephemeris. This could be facilitated if several stations are used simultaneously. In addition, a co-located GPS geodetic antenna and receiver would allow for an estimation of the tropospheric delay.

ACKNOWLEDMENT

REFERENCES

[1] T.E. Parker, V.S. Zhang, A. McKinley, L.M. Nelson, J. Rohde, and D. Matsakis, "Investigation of Instabilities in Two-Way Satellite Time and Frequency Transfer," Proc. 2002 PTTI Mtg., pp.381-390,, 2002.

[2] Jiang, G. Petit, "Combination of GPS Carrier Phase data with a calibrated time transfer link," Proc. 2007 Joint IEEE Freq. Cont. Symp. and European Time and Freq. Forum, pp.1182-1187, 2007.

[3] V. Zhang, T.E. Parker, M.A. Weiss, "Long-term comparisons of remote clocks with IGS clock products," Proc. 2007 PTTI Mtg., in publication.

[4] U.S. Coast Guard Navigation Center, on-line GPS Modernization page at http://www.navcen.uscg.gov/gps/modernization/default.htm

[5] Hopfield H.S., "Two-Quartic tropospheric refractivity profile for correcting satellite data," J. Geophys. Res.,74(18), 4487-4499, 1969.

[6] D.B. Sullivan, D.W. Allan, D.A. Howe, and F.L. Walls (ed.s), *Charcterization of Clocks and Oscillators*, NIST Tech. Note 1337, 1990.

[7] D. A. Howe, F Vernotte, "Generalization of the total variance approach to the modified Allan variance," Proc. 1999 PTTI Mtg., pp. 267-276, December 1999.

[8] D.W. Allan, M.A. Weiss, and J.L. Jespersen, "A Frequency-Domain View of Time-Domain Characterization of Clocks and Time and Frequency Distribution Systems," Proc. 1991 IEEE Freq. Cont. Symp., pp.667-678, 1991.

[9] T.E. Parker, D.A. Howe, and M.A. Weiss, "Accurate Frequency Comparisons at the 1 x 10^{-15} Level," Proc. 1998 IEEE Intl. Freq. Cont. Symp. pp.265-272, May 1998.

[10] M. Hottovy, M. Weiss, "Differential Delay Between Two Geodetic GPS Receivers for L1 and L2 Code and Carrier Signals," in these same Proc. 2008 IEEE Intl. Freq. Cont. Symp. 2008.
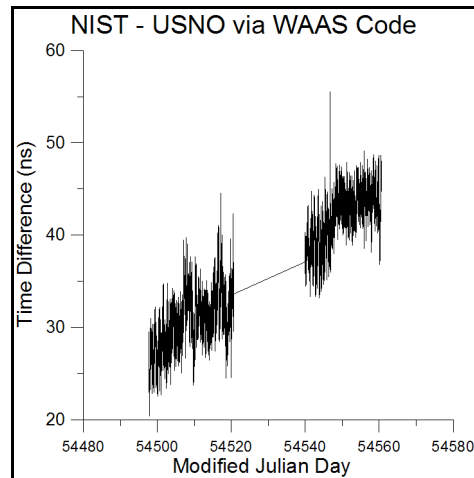
Figure 1. NIST minus USNO reference clocks using uncalibrated WAAS code data.
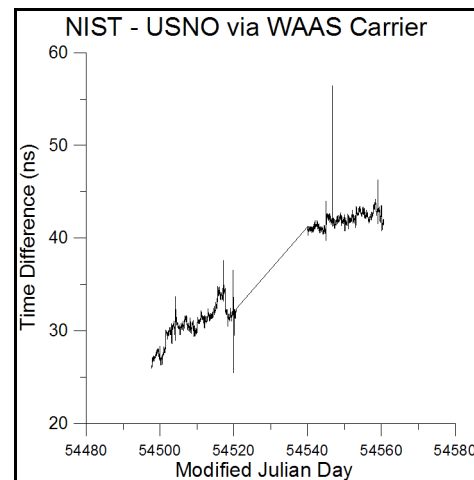

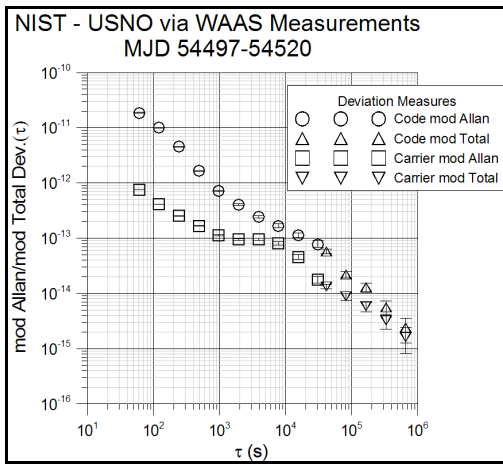Figure 2. NIST minus USNO reference clocks using uncalibrated WAAS carrier data.

Figure 3. Modified Allan and modified Total deviations of WAAS code and carrier measurements for the comparison of NIST minus USNO time scales, over the first segment in Figs. 1 and 2.
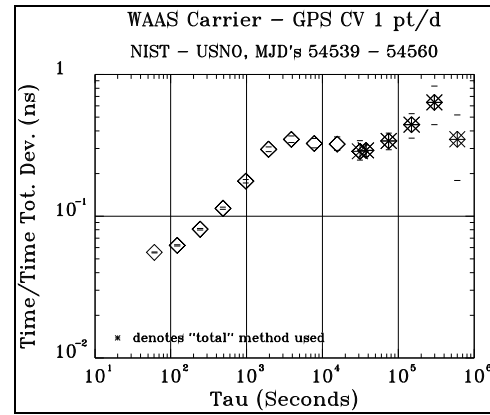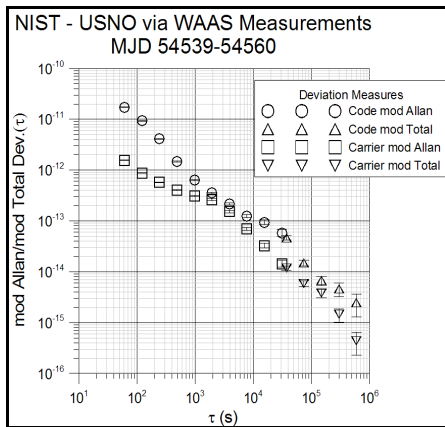

Figure 4. Modified Allan and modified Total deviations of WAAS code and carrier measurements for the comparison of NIST minus USNO time scales, over the second segment in Figs. 1 and 2.
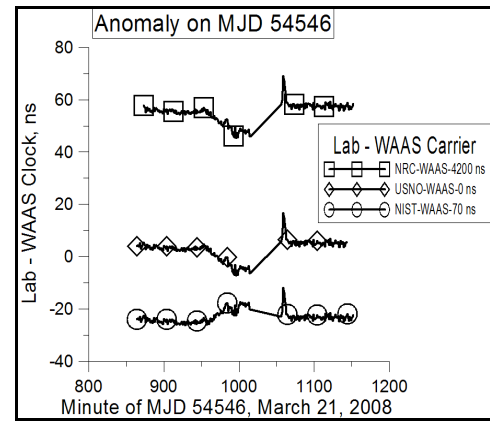

Figure 5. The difference of data from two time transfer systems for the NIST-USNO link. This is the WAAS carrier data as in Fig. 2 with GPS common-view (L1 code only) 1 d averages subtracted.
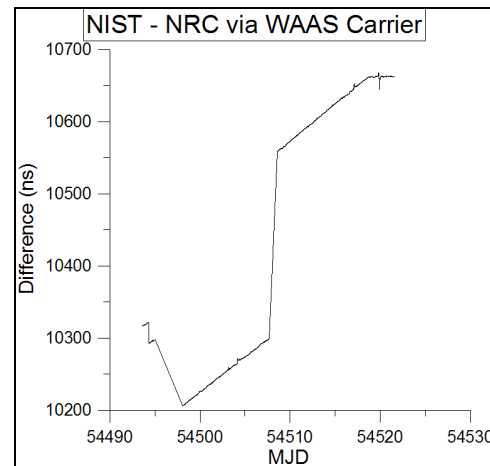

Figure 6. Time and time Total deviations of the data in the second segment of Fig. 5.

Figure 7. Detail of WAAS carrier measurements against individual labs showing the cause of the large spike in NIST-USNO data on MJD 54546.

Figure 8. NIST minus NRC reference clocks using uncalibrated WAAS carrier data. Several clock events prevent analysis of a long segment of data.
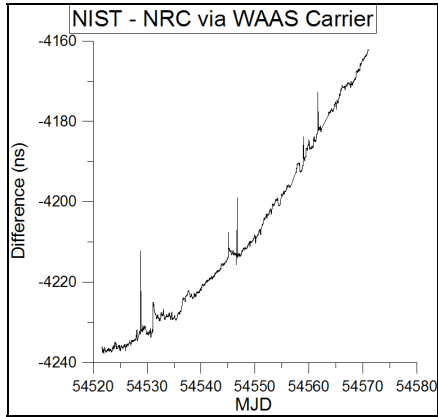
736

Figure 9. NIST minus NRC reference clocks using WAAS carrier data for the final segment of this study.
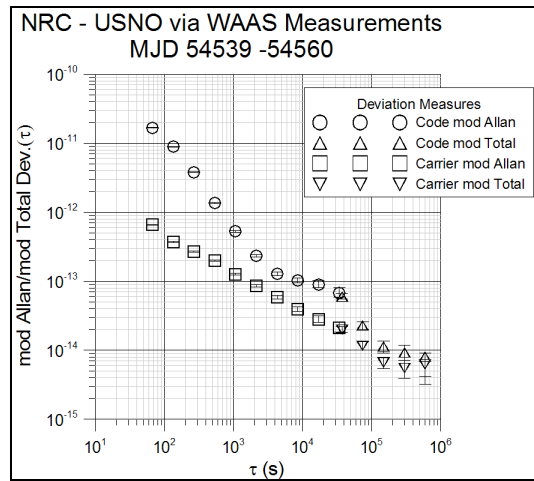

Figure 11. Modified Allan and modified Total deviations of WAAS code and carrier measurements for the comparison of NRC minus USNO time scales, over the last segment available in this study.
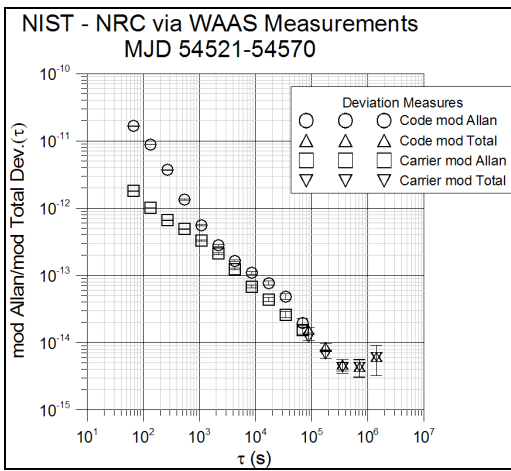

Figure 10. Modified Allan and modified Total deviations of WAAS code and carrier measurements for the comparison of NIST minus NRC time scales, over the segment in Fig. 9.